of these modes on the pulse broadening would be reduced to some extent.

References

[1] T. Uchida, M. Furukawa, I. Kitano, K. Koizumi, and H. Matsumura, "A light-focusing fiber guide," *IEEE J. Quantum Electron.*, vol. QE-5, p. 331, June 1969.

[2] D. Gloge, E. L. Chinnock, and K. Koizumi, "Study of pulse distortion in selfoc fibers," *Electron. Lett.*, vol. 8, pp. 526–527, Oct. 1072.

[3] Y. Suematsu and K. Furuya, "Refractive index distribution and group delay characteristics in multimode dielectric optical waveguides," *Trans. IECE Japan*, vol. 57-C, pp. 289–296, Sept. 1974.

[4] M. Matsuhara, "Analysis of TEM modes in dielectric waveguides by a variational method," *J. Opt. Soc. Amer.*, vol. 63, pp. 1514–1517, Dec. 1973.

[5] M. Geshiro, M. Ootaka, M. Matsuhara, and N. Kumagai, "Analysis of wave modes in slab waveguide with truncated parabolic index," *IEEE J. Quantum Electron.* (Corresp.), vol. QE-10, pp. 647–649, Sept. 1974.

[6] J. A. Stratton, *Electromagnetic Theory*. New York: McGraw-Hill, 1941, p. 343.

[7] P. M. Morse and H. Feshbach, *Methods of Theoretical Physics*. New York: McGraw-Hill, 1953, p. 1106.

Analysis of the Microstrip and the Electrooptic Light Modulator

MASANORI KOBAYASHI

Abstract—**Green's function for examples with anisotropic media is obtained using the image-coefficient method. The method is based on the boundary conditions and the reciprocity relation. Using this Green's function and solving directly the charge distribution on the strip, the line capacitances per unit length of a microstrip and of an electrooptic light modulator are obtained. High accuracy of this method is demonstrated by comparing the present results with the results obtained using the conformal mapping and with other data appeared in the literature. The charge distributions are also illustrated. Of particular interest is the effective filling fraction of the dielectric material, which depends mainly on the shape ratio and only slightly on the relative dielectric constant. The effective filling fractions are tabulated for the microstrip with a homogeneous dielectric substrate.**

List of Symbols

ε_0	Permittivity of free space (vacuum).
$\bar{\varepsilon}$	Permittivity tensor of anisotropic material.
ε_x^*, ε_y^*	Relative dielectric constants of anisotropic material in the directions of x-axis and y-axis, respectively.
ε^*	Relative dielectric constant of isotropic material.
$\varepsilon_{\text{eff}}^* = \dfrac{C/\varepsilon_0}{C_0/\varepsilon_0}$	Effective relative dielectric constant.
$q_w = \dfrac{\varepsilon_{\text{eff}}^* - 1}{\varepsilon^* - 1}$	Wheeler's effective filling fraction.
C	Capacitance per unit length of microstrip or of electrooptic light modulator.
C_0	Capacitance per unit length of line without dielectric.
q	Line charge.
σ	Charge distribution on the conductor.
m	Number dividing the conductor.
γ	Constant of 1, 2, or 3.
N	Truncated number of the infinite series in Green's function.
K	$= \dfrac{\sqrt{\varepsilon_{2x}^*\varepsilon_{2y}^*} - \sqrt{\varepsilon_{1x}^*\varepsilon_{1y}^*}}{\sqrt{\varepsilon_{2x}^*\varepsilon_{2y}^*} + \sqrt{\varepsilon_{1x}^*\varepsilon_{1y}^*}}$ image coefficient.
$\psi(q, \varepsilon_x^*, \varepsilon_y^*, \theta)$	Electric flux per unit angle emitted from the source line charge q in the radial direction with the angle θ from the x-axis.
α	$= \alpha_2/\alpha_1 (\alpha_1 = \sqrt{\varepsilon^*{}_{1y}/\varepsilon^*{}_{1x}}\ \alpha_2 = \sqrt{\varepsilon^*{}_{2y}/\varepsilon^*{}_{2x}}$.
$Z_c = \sqrt{\mu_0/\varepsilon_0}$	Intrinsic impedance of the free space (vacuum).

Manuscript received March 1, 1977; revised June 27, 1977.

The author is with the Department of Electrical Engineering, Faculty of Engineering, Ibaraki University, Hitachi, Ibaraki, 316 Japan.

I. Introduction

THE CALCULATION of the parameters of a microstrip line based on a TEM approximation is useful for the design of microwave integrated circuit structures [1]–[8]. The parameters can be derived from the line capacitance. The method in [1] is based on modified conformal mapping. The methods in [2], [3], [5]–[8] use Green's function satisfying the boundary conditions. The method in [4] is based on the relaxation technique. Isotropic substrate

0018-9480/78/0200-0119$00.75

materials are treated. On the other hand, the single-crystal sapphire with its well-defined and repeatable anisotropic properties is an attractive substrate material for microstrip circuits. Recently, the effect of anisotropy of the sapphire on the quasi-static characteristics of microstrip lines have been investigated by the finite difference method [9].

The electrooptic light modulators have received considerable attention [10]–[17]. The modulator made of an anisotropic crystal can impress the information onto the laser beam by means of the electrooptic effect in the crystal. The impedance and velocity matching which are principal limiting factors of the modulator bandwidth have been studied [13], [16], [17]. The characteristic impedance and phase velocity of the modulator can be derived from the line capacitance. The latter can be calculated by using Green's function. Therefore, the phase matching problems of the modulator are reduced to determining the Green's function for the boundary-value problems in the modulator.

Recently, the microstrip analysis based on the variational technique and Green's function was applied to the design of a broad-band electrooptic light modulator with rectangular side walls [16]. Subsequently, the line capacitance of a thin-film electrooptic light modulator with parallel-strip electrodes and with an anisotropic medium was calculated by the variational technique using Green's function in the Fourier-transformed domain [17].

It is the purpose of this paper to propose the method that has a high accuracy over a wide range of shape ratio of the strips to any anisotropic substrates and gives an accurate knowledge of the charge distribution on the strips. The method has academic interest in the numerical calculation. The other methods discussed in the literature have produced good approximations to the line capacitance because the line capacitance is variationally stationary. Hence, even relatively large errors in the computed charge distributions will yield acceptably good values of line capacitance for practical purposes. The substrip approximations [2], [5] and the projective method [7] can be expected to find good charge distribution. However, no method for producing an accurate charge distribution for any shape ratios and any dielectric materials containing anisotropic media has appeared in the literature. The Green's function for the examples with anisotropic media is determined by using the method derivable from the boundary conditions and the validity of the reciprocity relation satisfied by Green's function. It is an extension of the image-coefficient method reported in [2]. Using this Green's function and solving directly the charge distribution, we obtain the line capacitances per unit length of a microstrip and an electrooptic light modulator. These **closely** computed values are useful not only for testing simple approximate formulas but also for checking the accuracy of other available methods appeared in literature. The knowledge of the line capacitance is employed to calculate the characteristic impedance. The above results are compared with other available data. The charge distributions are illustrated in the figures. An accurate knowledge of the charge distribution becomes increasingly necessary [7] in analyzing discontinuity effects (open circuits, bends, and others). Of particular interest is the effective filling fraction q_w of the dielectric material proposed by Wheeler [1], which depends mainly on the shape ratio and only slightly on the relative dielectric constant. The effective filling fractions are tabulated for the microstrip with homogeneous dielectric substrate.

II. Image-Coefficient Method

Consider the two-dimensional space filled with only the medium of the following permittivity tensor:

$$\bar{\varepsilon} = \begin{pmatrix} \varepsilon_x & 0 \\ 0 & \varepsilon_y \end{pmatrix}, \qquad \varepsilon_x = \varepsilon_x^* \varepsilon_0, \qquad \varepsilon_y = \varepsilon_y^* \varepsilon_0 \tag{1}$$

where ε_x^* and ε_y^* are the relative dielectric constants and ε_0 is the permittivity of vacuum. Green's function $G(x, y; x_0, y_0)$ in space is defined as a solution of the two-dimensional inhomogeneous partial differential equation

$$\varepsilon_x^* \frac{\partial^2 G}{\partial x^2} + \varepsilon_y^* \frac{\partial^2 G}{\partial y^2} = -\frac{\delta(x - x_0)\delta(y - y_0)}{\varepsilon_0}. \tag{2}$$

Applying the coordinate transformation

$$X = \frac{x}{\sqrt{\varepsilon_x^*}}, \qquad Y = \frac{y}{\sqrt{\varepsilon_y^*}} \tag{3}$$

and the property of delta function

$$\delta(mx) = \delta(x)/|m| \tag{4}$$

to (2), we get

$$\frac{\partial^2 G}{\partial X^2} + \frac{\partial^2 G}{\partial Y^2} = -\frac{1}{\varepsilon_0 \sqrt{\varepsilon_x^* \varepsilon_y^*}} \delta(X - X_0)\delta(Y - Y_0). \tag{5}$$

Therefore, we can obtain the solution of (2) by applying (3) inversely to the solution of (5), that is

$$G(x, y; x_0, y_0) = \frac{1}{2\varepsilon_0 \sqrt{\varepsilon_x^* \varepsilon_y^*}} \cdot \ln \frac{c}{\sqrt{\frac{\varepsilon_y^*}{\varepsilon_x^*}(x - x_0)^2 + (y - y_0)^2}} \tag{6}$$

where c is a constant.

Next, consider the case (Fig. 1) of two anisotropic media of the following permittivity tensors:

$$\bar{\varepsilon}_1 = \begin{pmatrix} \varepsilon_{1x} & 0 \\ 0 & \varepsilon_{1y} \end{pmatrix}, \qquad \varepsilon_{1x} = \varepsilon_{1x}^* \varepsilon_0, \; \varepsilon_{1y} = \varepsilon_{1y}^* \varepsilon_0 \tag{7}$$

$$\bar{\varepsilon}_2 = \begin{pmatrix} \varepsilon_{2x} & 0 \\ 0 & \varepsilon_{2y} \end{pmatrix}, \qquad \varepsilon_{2x} = \varepsilon_{2x}^* \varepsilon_0, \; \varepsilon_{2y} = \varepsilon_{2y}^* \varepsilon_0. \tag{8}$$

We can define the Green's function $G(x, y; x_0, y_0)$ for the unit line charge per unit length $q_0 = 1$ at the source point $Q_0 = (x_0, y_0)$ as the solution satisfying the partial differential equation (2) with boundary conditions at $x = 0$

$$G|_{x=0_-} = G|_{x=0_+} \tag{9}$$

$$\varepsilon_{1x} \frac{\partial G}{\partial x}\bigg|_{x=0_-} = \varepsilon_{2x} \frac{\partial G}{\partial x}\bigg|_{x=0_+} \tag{10}$$

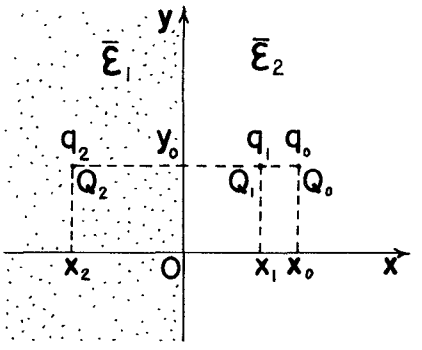

Fig. 1. Image charges of a line charge in the space with two anisotropic media.

and the reciprocity relation [20, eq. (9)]. We obtain the following results by using the image charges, q_1 at $Q_1 = (x_1, y_0)$ and q_2 at $Q_2 = (x_2, y_0)$, in (6):

$$G = \begin{cases} \dfrac{q_1}{2\pi\varepsilon_0\sqrt{\varepsilon_{1x}^*\varepsilon_{1y}^*}} \ln \dfrac{c_1}{\sqrt{\dfrac{\varepsilon_{1y}^*}{\varepsilon_{1x}^*}(x-x_1)^2 + (y-y_0)^2}}, \\ \qquad x \le 0 \quad (11) \\ \dfrac{q_0}{2\pi\varepsilon_0\sqrt{\varepsilon_{2x}^*\varepsilon_{2y}^*}} \ln \dfrac{c_2}{\sqrt{\dfrac{\varepsilon_{2y}^*}{\varepsilon_{2x}^*}(x-x_0)^2 + (y-y_0)^2}} \\ \quad + \dfrac{q_2}{2\pi\varepsilon_0\sqrt{\varepsilon_{2x}^*\varepsilon_{2y}^*}} \ln \dfrac{c_2}{\sqrt{\dfrac{\varepsilon_{2y}^*}{\varepsilon_{2x}^*}(x-x_2)^2 + (y-y_0)^2}}, \\ \qquad 0 \le x \quad (12) \end{cases}$$

where

$$c_1 = c_2 = 1 \quad (13)$$

$$x_1 = \sqrt{\frac{\varepsilon_{1x}^*}{\varepsilon_{1y}^*}}\sqrt{\frac{\varepsilon_{2y}^*}{\varepsilon_{2x}^*}}\, x_0 \quad (14)$$

$$x_2 = -x_0 \quad (15)$$

$$q_1 = (1-K)q_0 \quad (16)$$

$$q_2 = Kq_0 \quad (17)$$

$$K = \frac{\sqrt{\varepsilon_{2x}^*\varepsilon_{2y}^*} - \sqrt{\varepsilon_{1x}^*\varepsilon_{1y}^*}}{\sqrt{\varepsilon_{2x}^*\varepsilon_{2y}^*} + \sqrt{\varepsilon_{1x}^*\varepsilon_{1y}^*}}. \quad (18)$$

Next, consider the two-dimensional space filled with only the medium of permittivity tensor $\bar{\varepsilon}$ given by (1). The potential ϕ at an arbitrary point $r = (x,y)$ for the line charge q_0 at the source point $r_0 = (x_0, y_0)$ can be expressed from (6) and (13) as follows:

$$\phi = \frac{q_0}{2\pi\varepsilon_0\sqrt{\varepsilon_x^*\varepsilon_y^*}} \ln \frac{1}{\sqrt{\dfrac{\varepsilon_y^*}{\varepsilon_x^*}(x-x_0)^2 + (y-y_0)^2}}. \quad (19)$$

The electric flux density $\boldsymbol{D}$ is expressed as follows:

$$\boldsymbol{D} = \bar{\varepsilon} \cdot (-\nabla\phi) = \frac{q_0\sqrt{\varepsilon_x^*\varepsilon_y^*}\{(x-x_0)i + (y-y_0)j\}}{2\pi\{\varepsilon_x^*(y-y_0)^2 + \varepsilon_y^*(x-x_0)^2\}}. \quad (20)$$

Therefore, we find that the source charge emits the electric flux in the radial direction from (20), and the equipotential lines become the ellipses from (19), as illustrated in Fig. 2. Let the electric flux per unit angle emitted from the source charge in the radial direction with the angle $\theta(\le \pi/2)$ from the x-axis be denoted by $\psi(q_0, \varepsilon_x^*, \varepsilon_y^*, \theta)$, so that

$$\psi(q_0, \varepsilon_x^*, \varepsilon_y^*, \theta) = |r - r_0|\,|\boldsymbol{D}| = \frac{q_0}{2\pi}\frac{\sqrt{\varepsilon_x^*\varepsilon_y^*}}{\varepsilon_x^*\sin^2\theta + \varepsilon_y^*\cos^2\theta}. \quad (21)$$

Using this electric flux, the vectors, $\boldsymbol{D}$ and $\boldsymbol{E}$, can be expressed as follows:

$$\boldsymbol{D} = \psi(q_0, \varepsilon_x^*, \varepsilon_y^*, \theta)\frac{r - r_0}{|r - r_0|^2} \quad (22)$$

$$\boldsymbol{E} = \bar{\varepsilon}^{-1} \cdot \boldsymbol{D}. \quad (23)$$

Now, the Green's function for the case with the unit line charge at the point Q_0 as illustrated in Fig. 1 can be also obtained by the image-coefficient method shown below by illustrating the refraction and reflection of the flux $\psi(1, \varepsilon_{2x}^*, \varepsilon_{2y}^*, \theta_2)$ as shown in Fig. 3. At the interface, the y-axis, the fraction $K\psi(1, \varepsilon_{2x}^*, \varepsilon_{2y}^*, \theta_2)$ of the flux $\psi(1, \varepsilon_{2x}^*, \varepsilon_{2y}^*, \theta_2)$ emitted from the source point Q_0 reflects and goes as emitted from the image point Q_2, and the remainder $(1-K)\psi(1, \varepsilon_{1x}^*, \varepsilon_{1y}^*, \theta_1)$ refracts and goes as emitted from the image point Q_1. The boundary conditions at an arbitrary point B on the interface become as follows by using (22) and (23) from the requirements of continuity of the normal electric flux density component $\boldsymbol{D}_n$ and the tangential electric field component $\boldsymbol{E}_t$:

$$(1-K)\psi(1, \varepsilon_{1x}^*, \varepsilon_{1y}^*, \theta_1)\frac{\cos\theta_1}{r_{BQ_1}} = \psi(1, \varepsilon_{2x}^*, \varepsilon_{2y}^*, \theta_2) \cdot \frac{\cos\theta_2}{r_{BQ_0}} - K\psi(1, \varepsilon_{2x}^*, \varepsilon_{2y}^*, \theta_2) \cdot \frac{\cos\theta_2}{r_{BQ_2}} \quad (24)$$

$$\frac{1-K}{\varepsilon_{1y}}\psi(1, \varepsilon_{1x}^*, \varepsilon_{1y}^*, \theta_1)\frac{\sin\theta_1}{r_{BQ_1}} = \frac{1}{\varepsilon_{2y}}\psi(1, \varepsilon_{2x}^*, \varepsilon_{2y}^*, \theta_2) \cdot \frac{\sin\theta_2}{r_{BQ_0}} + \frac{K}{\varepsilon_{2y}}\psi(1, \varepsilon_{2x}^*, \varepsilon_{2y}^*, \theta_2) \cdot \frac{\sin\theta_2}{r_{BQ_2}} \quad (25)$$

where r_{BQ} denotes the distance between the points B and Q. The boundary conditions (24) and (25) are satisfied by

$$r_{BQ_1}\cos\theta_1 = \sqrt{\frac{\varepsilon_{1x}^*}{\varepsilon_{1y}^*}}\sqrt{\frac{\varepsilon_{2y}^*}{\varepsilon_{2x}^*}}\, r_{BQ_0}\cos\theta_2 \quad (26)$$

$$K = \frac{\sqrt{\varepsilon_{2x}^*\varepsilon_{2y}^*} - \sqrt{\varepsilon_{1x}^*\varepsilon_{1y}^*}}{\sqrt{\varepsilon_{2x}^*\varepsilon_{2y}^*} + \sqrt{\varepsilon_{1x}^*\varepsilon_{1y}^*}}. \quad (27)$$

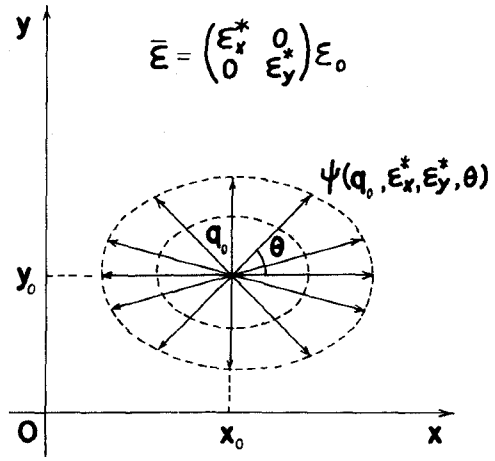

Fig. 2. Electric flux and equipotential line for a line charge in the anisotropic medium.

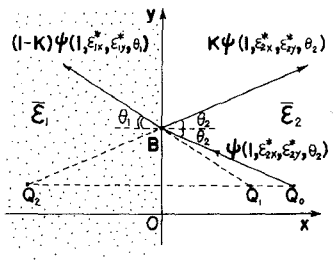

Fig. 3. Refraction and reflection of the flux $\psi(1, \varepsilon_{2x}^*, \varepsilon_{2y}^*, \theta_2)$ emitted from a unit line charge in the space with anisotropic media.

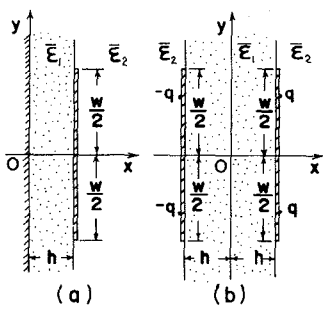

Fig. 4. Microstrip line. (a) Microstrip line. (b) Electrostatically equivalent-2 ribbon line.

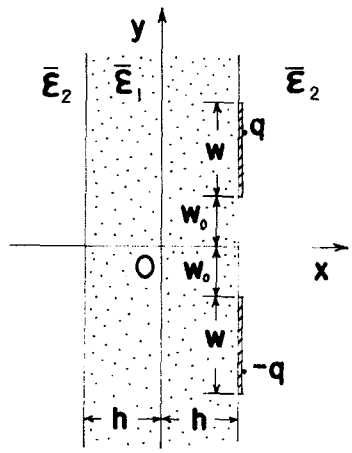

Fig. 5. Electrooptic light modulator line.

Then, we find that (26) and (27) are identical to (14)–(18). Therefore, the Green's function can be obtained as (11) and (12) by using the image charges, $(1 - K)$ at the point Q_1, and K at the point Q_2.

III. Green's Function

The parameters, a characteristic impedance Z, a phase velocity v, and a guide wavelength λ, for the microstrip (Fig. 4) and for the electrooptic light modulator (Fig. 5) can be obtained from the line capacitance C between the conductors as follows:

$$Z = 1/(v_0\sqrt{CC_0}) \tag{28}$$

$$v = v_0\sqrt{C_0/C} \tag{29}$$

$$\lambda = \lambda_0\sqrt{C_0/C} \tag{30}$$

where v_0 denotes the velocity of light, λ_0 the free space wavelength, and C_0 the line capacitance for the case of $\bar{\varepsilon}_1 = \bar{\varepsilon}_2 =$ vacuum. As the line capacitance can be calculated by using the Green's function, the problem is that we determine the Green's function. The Green's function for both the microstrip and the electrooptic light modulator can be determined as follows by illustrating the refraction and reflection of the electric flux emitted from the unit line charge at the source point $(h + d, y_0)$ using the image-coefficient method as shown in Fig. 6:

$$G(x, y; h+d, y_0) = \frac{1-K^2}{2\pi\varepsilon_0\sqrt{\varepsilon_{2x}^*\varepsilon_{2y}^*}} \sum_{n=0}^{\infty} K^{2n} \ln \frac{1}{\sqrt{\alpha_2^2\left[x - \left\{d + \frac{h}{\alpha}(2(2n+1) - \alpha\right\}\right]^2 + (y-y_0)^2}}, \qquad x \le -h \tag{31}$$

$$G(x, y; h+d, y_0) = \frac{1-K}{2\pi\varepsilon_0\sqrt{\varepsilon_{1x}^*\varepsilon_{1y}^*}} \sum_{n=0}^{\infty} \left[K^{2n} \ln \frac{1}{\sqrt{\alpha_1^2[x - \{(4n+1)h + \alpha d\}]^2 + (y-y_0)^2}}\right.$$
$$\left. - K^{2n+1} \ln \frac{1}{\sqrt{\alpha_1^2[x + \{(4n+3)h + \alpha d\}]^2 + (y-y_0)^2}}\right], \qquad -h \le x \le h \tag{32}$$

$$G(x, y; h+d, y_0) = \frac{1}{2\pi\varepsilon_0\sqrt{\varepsilon_{2x}^*\varepsilon_{2y}^*}} \left[\ln \frac{1}{\sqrt{\alpha_2^2\{x - (h+d)\}^2 + (y-y_0)^2}} + K \ln \frac{1}{\sqrt{\alpha_2^2\{x - (h-d)\}^2 + (y-y_0)^2}}\right.$$
$$\left. - \sum_{n=0}^{\infty} K^{2n+1}(1-K)^2 \ln \frac{1}{\sqrt{\alpha_2^2\left[x + \left\{d + \frac{h}{\alpha}(4(n+1) - \alpha)\right\}\right]^2 + (y-y_0)^2}}\right], \qquad h \le x \tag{33}$$

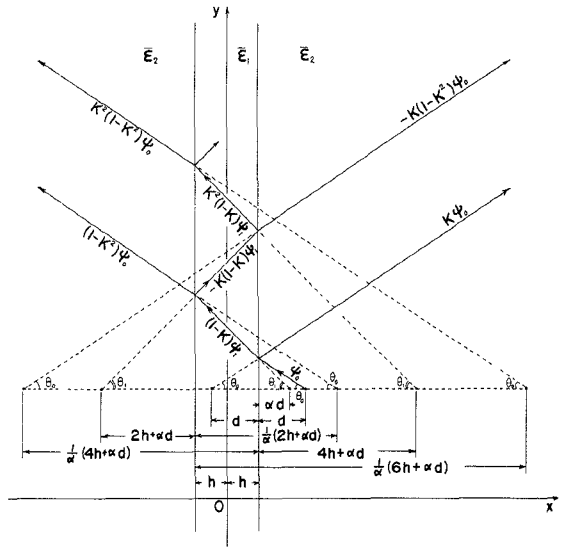

Fig. 6. Determination of multiple images of a unit line charge by the image-coefficient method. $\psi_0 \equiv \psi_0(1, \varepsilon^*_{2x}, \varepsilon^*_{2y}, \theta_0)$, $\psi_1 \equiv \psi_1(1, \varepsilon^*_{1x}, \varepsilon^*_{1y}, \theta_1)$.

where

$$K = \frac{\sqrt{\varepsilon^*_{2x}\varepsilon^*_{2y}} - \sqrt{\varepsilon^*_{1x}\varepsilon^*_{1y}}}{\sqrt{\varepsilon^*_{2x}\varepsilon^*_{2y}} + \sqrt{\varepsilon^*_{1x}\varepsilon^*_{1y}}},$$

$$\alpha = \frac{\alpha_2}{\alpha_1}, \qquad \alpha_1 = \sqrt{\frac{\varepsilon^*_{1y}}{\varepsilon^*_{1x}}}, \quad \text{and} \quad \alpha_2 = \sqrt{\frac{\varepsilon^*_{2y}}{\varepsilon^*_{2x}}}.$$

IV. Capacitance for Microstrip

The line capacitance per unit length C of the microstrip shown in Fig. 4(a) can be calculated as below if the charge quantity Q on the conductor in quadrant I can be obtained. Let us consider only quadrant I, due to symmetry, as the region for the boundary-value problem. Now, we can consider the image charges, $-q$, $-q$, and q, in quadrants II, III, and IV, respectively, as those of the line charge q at the source point (h,y_0) in the quadrant I as shown in Fig. 4(b). Then, the value of the Green's function at the point (h,y) on the conductor in quadrant I for $q = 1$ is determined as follows by the use of (31) and (33) for the electrostatically equivalent-2 ribbon line (Fig. 4(b)):

$$G(h, y; h, y_0) = \frac{1}{2\pi\varepsilon_0\left(\sqrt{\varepsilon^*_{2x}\varepsilon^*_{2y}} + \sqrt{\varepsilon^*_{1x}\varepsilon^*_{1y}}\right)} \sum_{n=1}^{\infty} K^{n-1} \cdot \ln \frac{\left\{4n^2 + \left(\frac{y-y_0}{\alpha_1 h}\right)^2\right\}\left\{4n^2 + \left(\frac{y+y_0}{\alpha_1 h}\right)^2\right\}}{\left\{4(n-1)^2 + \left(\frac{y-y_0}{\alpha_1 h}\right)^2\right\}\left\{4(n-1)^2 + \left(\frac{y+y_0}{\alpha_1 h}\right)^2\right\}}. \tag{34}$$

Here, let us express the desired unknown charge distribution $\sigma(h,y_0)$ on the conductor in quadrant I as shown in Fig. 7, so that the potential V at the point (h,y) on the conductor is expressed by the Green's function technique [20, eq. (20)] as follows:

$$V = \sum_{j=1}^{m} \int_{y_j}^{y_{j+1}} \sigma(h, y_0) G(h, y; h, y_0)\, dy_0 \tag{35}$$

$$\sigma(h, y_0) = \sigma_j + (\sigma_{j+1} - \sigma_j)\frac{y_0 - y_j}{y_{j+1} - y_j} \tag{36}$$

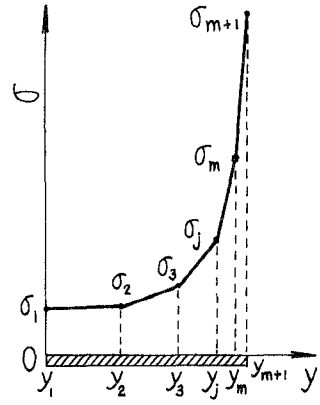

Fig. 7. Desired unknown charge distribution on the conductor in quadrant I for the microstrip.

where we take that

$$y_j = \frac{w}{2}\left\{1 - \left(1 - \frac{j-1}{m}\right)^{\gamma}\right\}, \qquad j = 1, 2, \cdots, m+1 \tag{37}$$

in order to make $\sigma(h,y_0)$ approach the true charge distribution, where γ is a constant of 1, 2, or 3. The potential V_k at each point (h,y_k) $(k = 1, 2, \cdots, m+1)$ on the conductor is expressed as follows by carrying out the integration of (35) and rearranging those results:

$$V_k = \sum_{j=1}^{m+1} p_{kj}\sigma_j, \qquad k = 1, 2, \cdots, m+1. \tag{38}$$

Solving the simultaneous equations (38) by letting V_k be the given potential of the conductor, V_0, we obtain σ_j giving the desired unknown quantity $\sigma(h,y_0)$. As the charge quantity Q on the conductor can be calculated by

$$Q = \sum_{j=1}^{m} \int_{y_j}^{y_{j+1}} \sigma(h,y_0)\, dy_0 \tag{39}$$

we obtain the line capacitance C of the microstrip as follows:

$$C = \frac{2Q}{V_0}. \tag{40}$$

The infinite series in (34) converge quickly; the detailed discussion on the convergence is shown by Silvester [2] for $\varepsilon_{1x} = \varepsilon_{1y} = \varepsilon_1$ and $\varepsilon_{2x} = \varepsilon_{2y} = \varepsilon_0$. In this paper, we take that $\varepsilon^*_{2x} = \varepsilon^*_{2y} = 1$. Table I shows the numerical results of the line capacitance C_0/ε_0 for $\varepsilon^*_{1x} = \varepsilon^*_{1y} = 1$ and the effective filling fraction q_w for $\varepsilon^*_{1x} = \varepsilon^*_{1y} = \varepsilon^*_1$. We took $m = 40$ as the divided number in (35), (38), and (39), $N = 50$ as the truncated number of the infinite series (34), and $\gamma = 3$ in (37). We took $N = 1, 100, 600$ for $\varepsilon^*_1 = 1, 16, 128$, respectively. It is checked with the larger divided number m that the results are greater

TABLE I
LINE CAPACITANCE PER UNIT LENGTH C_0/ε_0 AND EFFECTIVE FILLING FRACTION q_w OF MICROSTRIP WITH ISOTROPIC SUBSTRATE

ε_1^* / w/h	C_0/ε_0	Effective filling fraction q_w						
	1	1.01	1.5	2	4	8	16	128
0.01	0.939969	0.561680	0.547367	0.544902	0.540740	0.538629*	0.537441*	0.536800#
0.04	1.18587	0.565312	0.560106	0.557151	0.552236	0.549502	0.547960	0.546771*
0.10	1.43375	0.578900	0.573016	0.569632	0.563975	0.560825	0.559150	0.557641*
0.20	1.70270	0.593607	0.587092	0.583321	0.576983	0.573437	0.571548	0.569699
0.40	2.09393	0.614680	0.607485	0.603295	0.596207	0.592215	0.590082	0.587837
0.70	2.56365	0.638960	0.631299	0.626811	0.619174	0.614845	0.612523	0.610393
1.00	2.97991	0.659094	0.651269	0.646668	0.638808	0.634334	0.631929	0.629708
2.00	4.23158	0.710090	0.702537	0.698071	0.690398	0.686004	0.683634	0.681456
4.00	6.52698	0.772544	0.766173	0.762402	0.755913	0.752192	0.750183	0.748329
7.00	9.79686	0.823842	0.818821	0.815854	0.810758	0.807840	0.806266	0.804816
10.00	12.9814	0.854113	0.849977	0.847538	0.843356	0.840967	0.839679	0.838494
20.00	23.3628	0.903768	0.901149	0.899611	0.896985	0.895491	0.894687	0.893950
40.00	43.7668	0.939854	0.938327	0.937433	0.935914	0.935054	0.934591	0.934168
100.00	104.323	0.969596	0.968909	0.968082	0.967830	0.967447	0.967242	0.967055

$\varepsilon_{1x}^* = \varepsilon_{1y}^* = \varepsilon_1^*$, $\varepsilon_{2x}^* = \varepsilon_{2y}^* = 1$, m = 40, N = 50(N = 1, 100, 600 for ε_1^* = 1, 16, 128, respectively), γ = 3(γ = 1 for # and γ = 2 for *),
$q_w = (\varepsilon_{eff}^*-1)/(\varepsilon_1^*-1)$, $\varepsilon_{eff}^* = (C/\varepsilon_0)/(C_0/\varepsilon_0)$

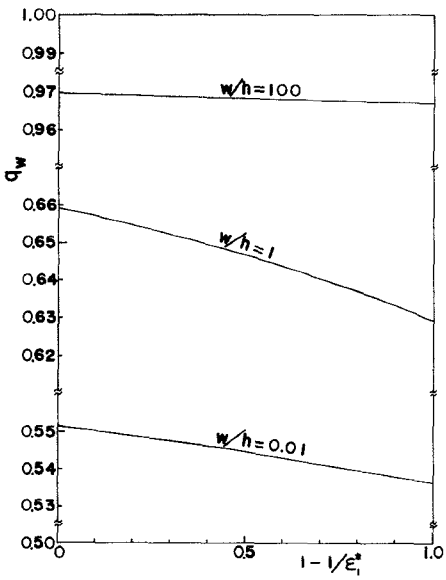

Fig. 8. Effective filling fraction of the microstrip.

than the true values. Comparing these results with the true values C_0/ε_0 obtained by the author using the conformal mapping [18], [19], shown in Table A-I, we find that the errors of the results C_0/ε_0 are less than +0.0024 percent for $w/h = 0.01$ and less than +0.001 percent for $w/h > 0.01$. The order of errors of C/ε_0 for $\varepsilon_1^* \neq 1$ is the same to that of C_0/ε_0 if we take N as follows:

$$K^{N-1} \ln\left(\frac{N}{N-1}\right)^4 < 10^{-6}. \tag{41}$$

The q_w is determined by Wheeler [1] and can be obtained from C/ε_0 as follows:

$$q_w = \frac{\varepsilon_{eff}^* - 1}{\varepsilon_1^* - 1}, \qquad \varepsilon_{eff}^* = (C/\varepsilon_0)/(C_0/\varepsilon_0). \tag{42}$$

Therefore, q_w, shown in Table I, are possible to a surprisingly high accuracy as the order of errors of C/ε_0 is the same to that of C_0/ε_0. We find that the q_w depends mainly on the shape ratio w/h and only slightly on the relative dielectric constant ε_1^* from Table I. If we draw q_w versus $(1 - 1/\varepsilon_1^*)$, we find that q_w changes almost linearly, the largest slope is for w/h = about 1.2. The q_w approaches 0.5 and its slope approaches zero when $w/h \to 0$. The q_w approaches 1 and its slope approaches zero when $w/h \to \infty$. Fig. 8 shows q_w for $w/h = 0.01$, 1, 100.

Table II shows the numerical results of C/ε_0 of the microstrips with sapphire substrate of anisotropic property. In Table III, the ratios Z/Z_c of the characteristic impedance Z of the microstrip to the intrinsic impedance Z_c of the free space (method A) are compared with those calculated by the author using Wheeler's formulas [1] (method B). We calculated the Z/Z_c of method A by using the results C_0/ε_0 and q_w in Table I as follows:

$$Z/Z_c = \frac{1}{\frac{C_0}{\varepsilon_0}\sqrt{\varepsilon_{eff}^*}}, \qquad \varepsilon_{eff}^* = 1 + q_w(\varepsilon_1^* - 1). \tag{43}$$

TABLE II
LINE CAPACITANCE PER UNIT LENGTH C/ε_0 OF MICROSTRIP WITH SAPPHIRE SUBSTRATE

ε_{1x}^* / ε_{1y}^* / w/h	9.4	11.6	11.6	9.4
0.1	8.78424		9.25962	
1.0	19.6889		22.0162	
10.0	105.506		127.628	

$\varepsilon_{2x}^* = \varepsilon_{2y}^* = 1$, m = 40, N = 50, γ = 3

TABLE III
RATIO Z/Z_c OF CHARACTERISTIC IMPEDANCE OF MICROSTRIP TO INTRINSIC IMPEDANCE OF FREE SPACE

ε_1^* / w/h		1	4	16	128
0.01	A	1.06386	0.656979	0.353413	0.127913
	B	1.06388	0.657402	0.353671	0.128046
1.00	A	0.335580	0.196503	0.103666	0.0372929
	B	0.335926	0.196998	0.103982	0.0374042
4.00	A	0.153210	0.0847546	0.0437694	0.0156338
	B	0.154007	0.0844588	0.0434946	0.0155191
100.00	A	0.00958559	0.00485168	0.00243406	0.000861451
	B	0.00958690	0.00485178	0.00243397	0.000861397

Method A: the method of this paper
Method B: the modified conformal mapping[1]

The ratios Z/Z_c are larger than the true values and the order of its errors is the same to that of C_0/ε_0. Comparing both methods, method B has a high accuracy for extremely wide and narrow strips as having been mentioned by Wheeler [1] and has a good accuracy for the intermediate strips. Method A has a high accuracy as mentioned above. Its reason is that the charge distributions can be obtained remarkably well.

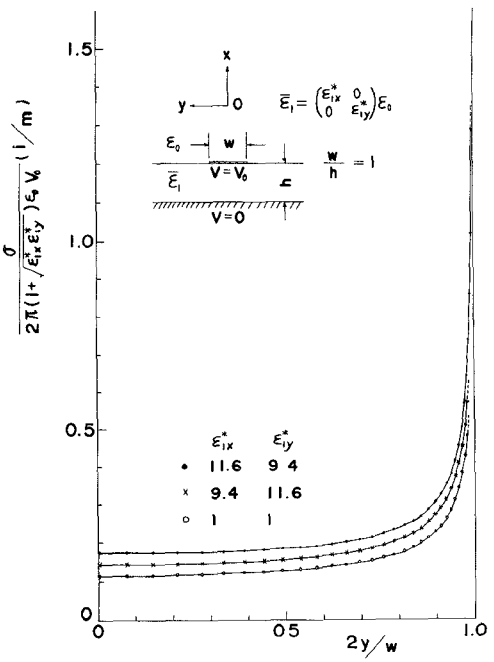

Fig. 9. Charge distributions obtained for the microstrip.

As an example, we show in Fig. 9 the charge distributions for sapphire substrates and for vacuum.

V. Capacitance for Electrooptic Light Modulator

The line capacitance per unit length of the electrooptic light modulator (Fig. 5) can be calculated by a method similar to that for the microstrip. The value of the Green's function, used then, at the point (h,y) on the conductor in the upper half region is expressed as follows:

$$G(h, y; h, y_0) = \frac{1}{2\pi\varepsilon_0\left(\sqrt{\varepsilon^*_{2x}\varepsilon^*_{2y}} + \sqrt{\varepsilon^*_{1x}\varepsilon^*_{1y}}\right)} \sum_{n=1}^{\infty} K^{n-1} \cdot \ln \frac{4(n-1)^2 + \left(\frac{y+y_0}{\alpha_1 h}\right)^2}{4(n-1)^2 + \left(\frac{y-y_0}{\alpha_1 h}\right)^2}. \quad (44)$$

Also, we express the desired unknown charge distribution $\sigma(h,y_0)$ on the conductor as follows:

$$\sigma(h,y_0) = \sigma_j + (\sigma_{j+1} - \sigma_j)\frac{y_0 - y_j}{y_{j+1} - y_j} \quad (45)$$

where we take that

$$y_j = \begin{cases} \left(w_0 + \frac{w}{2}\right) - \frac{w}{2}\left\{1 - \left(1 - \frac{s+1-j}{s}\right)v\right\}, \\ \qquad j = 1, 2, \cdots, s \left(s = \frac{m}{2}\right) \\ \left(w_0 + \frac{w}{2}\right) + \frac{w}{2}\left\{1 - \left(1 + \frac{s+1-j}{s}\right)v\right\}, \\ \qquad j = s+1, s+2, \cdots, m+1 \end{cases} \quad (46)$$

TABLE IV
Line Capacitance per Unit Length of Electrooptic Light Modulator with $LiNbO_3$ and Without

			$2w_0$[μm] 2	20	50	100	200	400
C_0/ε_0	$\varepsilon^*_{1x}=1$, $\varepsilon^*_{1y}=1$	C	3.30662	1.95071	1.50681	1.23317	1.01637	0.850136
		D	3.30586	1.95060	1.50675	1.23313	1.01635	0.850121
C/ε_0	$\varepsilon^*_{1x}=43$, $\varepsilon^*_{1y}=28$	C	59.0312	34.8300	26.9107	22.0372	18.1928	15.2915

2h = 2[μm], w = 44[μm], $\varepsilon^*_{2x} = \varepsilon^*_{2y} = 1$, m = 40,
N = 50 (N = 1 for $\varepsilon^*_{1x} = \varepsilon^*_{1y} = 1$), γ = 3,
Method C. the method of this paper
Method D: the conformal mapping

in order to make $\sigma(h,y_0)$ approach the true charge distribution, where γ is a constant of 1, 2, or 3.

Table IV shows the numerical results of the line capacitances per unit length C/ε_0 and C_0/ε_0 of the electrooptic light modulator lines with $LiNbO_3$ ($\varepsilon^*_{1x} = 43$, $\varepsilon^*_{1y} = 28$) and without. In Table IV, method C is that of this paper and method D is that of the conformal mapping. Here, we take that $2h = 2$ mm, $w = 44$ μm, and $\varepsilon^*_{2x} = \varepsilon^*_{2y} = 1$. It is checked with the larger m that the results obtained by method C are greater than the true values. Comparing the results with the true values obtained by method D, we find that the errors of method C for $\varepsilon^*_{1x} = \varepsilon^*_{1y} = 1$ are less than $+0.023$ percent for $2\ \mu\text{m} \le 2w_0 \le 400\ \mu\text{m}$. The order of errors of C/ε_0 for $LiNbO_3$ is the same to that of C_0/ε_0 if we take N as follows:

$$K^{N-1} \ln \frac{4(N-1)^2 + \left\{\frac{2(w+w_0)}{\alpha_1 h}\right\}^2}{4(N-1)^2} < 10^{-6}. \quad (47)$$

Yamashita and Atsuki [17] calculated C by the variational technique using Green's function. Comparing their results with our results in Table IV, for $w = 44$ μm, we find that their results are smaller by $4 \sim 10$ percent.

Method C has a high accuracy because the charge distributions can be obtained remarkably well as shown, for example, in Fig. 10. Although not shown here, it is worth pointing out that the charge distributions for $\varepsilon^*_{1x} = \varepsilon^*_{1y} = 1$ are nearly in agreement with and slightly less than those for $\varepsilon^*_{1x} = 43$ and $\varepsilon^*_{1y} = 28$ if both results are drawn by the same scales to those of Fig. 10. It means that the effective relative dielectric constant of the electrooptic light modulator with $LiNbO_3$ is about $(1 + \sqrt{\varepsilon^*_{1x}\varepsilon^*_{1y}})/2$ ($\doteqdot 17.849$).

VI. Conclusion

The Green's function for the examples with anisotropic media has been obtained using the image-coefficient method based on the boundary conditions and the reciprocity relation. Using this Green's function, the line capacitances per unit length of a microstrip and an electrooptic light modulator have been calculated with the aid of the digital computer, HITAC 8250 and HITAC 8800/8700. In order to demonstrate the high accuracy of the present method, the numerical results have been compared with the true values

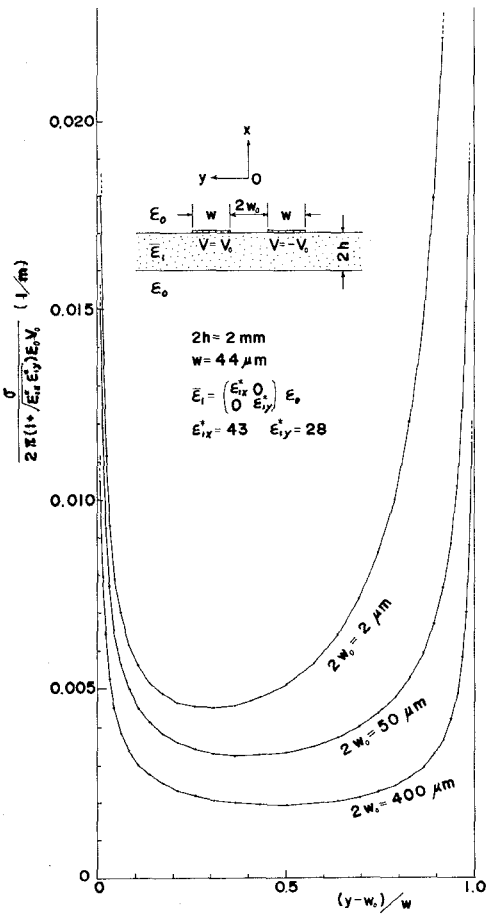

Fig. 10. Charge distributions obtained for the electrooptic light modulator.

TABLE A-I
TRUE LINE CAPACITANCE PER UNIT LENGTH OF MICROSTRIP WITHOUT SUBSTRATE

w/h	C_0/ε_0	w/h	C_0/ε_0	w/h	C_0/ε_0
0.01	0.939947	0.1	1.43375	1	2.97989
0.02	1.04869	0.2	1.70270	2	4.23155
0.03	1.12480	0.3	1.91198	3	5.39883
0.04	1.18587	0.4	2.09392	4	6.52694
0.05	1.23800	0.5	2.25993	5	7.63141
0.06	1.28412	0.6	2.41548	6	8.71990
0.07	1.32588	0.7	2.56364	7	9.79678
0.08	1.36431	0.8	2.70633	8	10.8648
0.09	1.40010	0.9	2.84479	9	11.9259
				10	12.9813

computed by the author using conformal mapping[18],[19]

obtained by conformal mapping and with other results published in literature and the charge distributions have been illustrated in the figures. The effective filling fractions have been tabulated.

Further work is in progress to calculate the parameters of the structures with the conductors of finite thickness and to propose the closely approximate formulas of C/ε_0 to be useful in the design of a microstrip and of an electrooptic light modulator.

APPENDIX

The line capacitance C_0/ε_0 per unit length of the microstrip can be found analytically by conformal mapping [18], [19], and the results calculated by the author are shown in Table A-I.

ACKNOWLEDGMENT

The author would like to thank Dr. R. Terakado for helpful discussions and guidance in numerical calculations and the use of conformal mapping. He would also like to thank the reviewers for helpful comments and the valuable suggestion with respect to the use of the effective filling fraction.

REFERENCES

[1] H. A. Wheeler, "Transmission-like properties of parallel strips separated by a dielectric sheet," *IEEE Trans. Microwave Theory Tech.*, vol. MTT-13, pp. 172–185, Mar. 1965.
[2] P. Silvester, "TEM wave properties of microstrip transmission lines," *Proc. IEE* (London), vol. 115, pp. 43–48, Jan. 1968.
[3] E. Yamashita and R. Mittra, "Variational method for the analysis of microstrip lines," *IEEE Trans. Microwave Theory Tech.*, vol. MTT-16, pp. 251–256, Apr. 1968.
[4] H. E. Stinehelfer, Sr., "An accurate calculation of uniform microstrip transmission lines," *IEEE Trans. Microwave Theory Tech.*, vol. MTT-16, pp. 439–444, July 1968.
[5] T. G. Bryant and J. A. Weiss, "Parameters of microstrip transmission lines and of coupled pairs of microstrip lines," *IEEE Trans. Microwave Theory Tech.*, vol. MTT-16, pp. 1021–1027, Dec. 1968.
[6] R. Mittra and T. Itoh, "Charge and potential distributions in shielded striplines," *IEEE Trans. Microwave Theory Tech.*, vol. MTT-18, pp. 149–156, Mar. 1970.
[7] P. Silvester and P. Benedek, "Electrostatics of the microstrip—Revised," *IEEE Trans. Microwave Theory Tech.* (Short Papers), vol. MTT-20, pp. 756–758, Nov. 1972.
[8] A. Farrar and A. T. Adams, "Multilayer microstrip transmission lines," *IEEE Trans. Microwave Theory Tech.* (Short Papers), vol. MTT-22, pp. 889–891, Oct. 1974.
[9] R. P. Owens, J. E. Aitken, and T. C. Edwards, "Quasi-static characteristics of microstrip on an anisotropic sapphire substrate," *IEEE Trans. Microwave Theory Tech.*, vol. MTT-24, pp. 499–505, Aug. 1976.
[10] I. P. Kaminow and E. H. Turner, "Electrooptic light modulator," *Proc. IEEE*, vol. 54, pp. 1374–1390, Oct. 1966.
[11] F.-S. Chen, "Modulators for optical communications," *Proc. IEEE*, vol. 58, pp. 1440–1457, Oct. 1970.
[12] G. White, "A one-gigabit-per-second optical PCM communications system," *Proc. IEEE* (Lett.), vol. 58, pp. 1779–1780, Oct. 1970.
[13] E. Yamashita and K. Atsuki, "A proposed microwave structure and design method for the traveling-wave modulation of light," *IEEE Trans. Microwave Theory Tech.* (Corresp.), vol. MTT-17, pp. 118–119, Feb. 1969.
[14] I. P. Kaminow and J. R. Carruthers, "Optical waveguiding layers in $LiNbO_3$ and $LiTaO_3$," *Appl. Phys. Lett.*, vol. 22, pp. 326–328, Apr. 1973.
[15] I. P. Kaminow, J. R. Carruthers, E. H. Turner, and L. W. Stulz, "Thin-film $LiNbO_3$ electro-optic light modulator," *Appl. Phys. Lett.*, vol. 22, pp. 540–542, May 1973.
[16] E. Yamashita, K. Atsuki, and T. Akamatsu, "Application of microstrip analysis to the design of a broad-band electrooptical modulator," *IEEE Trans. Microwave Theory Tech.* (Short Papers), vol. MTT-22, pp. 462–464, Apr. 1974.
[17] E. Yamashita and K. Atsuki, "Distributed capacitance of a thin-film electrooptic light modulator," *IEEE Trans. Microwave Theory Tech.* (Lett.), vol. MTT-23, pp. 177–178, Jan. 1975.
[18] H. B. Palmer, "The capacitance of a parallel-plate capacitor by the Schwartz-Christoffel transformation," *Trans. Amer. Inst. Elect. Eng.*, vol. 56, pp. 363–366, 1937.
[19] K. G. Black and T. J. Higgins, "Rigorous determination of the parameters of microstrip transmission lines," *IRE Trans. Microwave Theory Tech.*, vol. MTT-3, pp. 93–113, 1955.
[20] M. Kobayashi, "Green's function technique for solving anisotropic electrostatic field problems," *IEEE Trans. Microwave Theory Tech.*, to be submitted.